UCLA

Berkeley Lab

Berkeley
UNIVERSITY OF CALIFORNIA

Accessing **Saturation** and **Sub-Nuclear Structure** with Multiplicity Dependent J/ψ production in p+p and p+Pb Collisions

INSTITUTE for NUCLEAR THEORY

Farid Salazar

Based on
arXiv *2112.04611*
[PLB 827 (2022) 136952]

+ work in progress

In collaboration with

Björn Schenke (BNL), and
Alba Soto-Ontoso (IPhT Saclay → CERN)

Outline

- Quarkonium production in pp and pA
- Sub-nuclear fluctuations
- Quarkonium production in eA
- Summary

Quarkonium production in pp and pA

Kinematics of quarkonium production

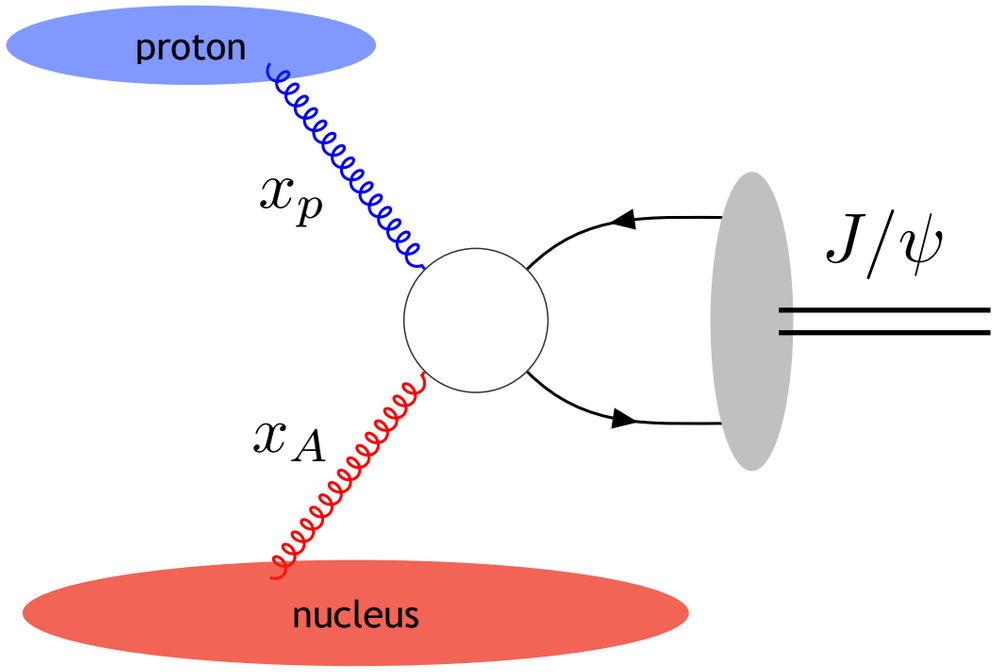

$$x_p = \sqrt{\frac{M^2_{J/\Psi} + P^2_\perp}{s}} e^{Y}$$

$$x_A = \sqrt{\frac{M^2_{J/\Psi} + P^2_\perp}{s}} e^{-Y}$$

- Large energy limit $s \longrightarrow \infty$

$$x_p, x_A \ll 1$$

- Asymmetric kinematics:

Forward production $Y \gg 1 \longrightarrow x_p \sim 1, x_A \ll 1$

Backward production $Y \ll -1 \longrightarrow x_p \ll 1, x_A \sim 1$

Need to account for:

(1) Multiple scatterings due to high parton densities at low-x
(2) Resummation of energy logs $\ln(s) \propto \ln(1/x_{p/A})$

Quarkonium production in pp and pA

The Color Glass Condensate in a Nutshell: anatomy of QCD at high-energy

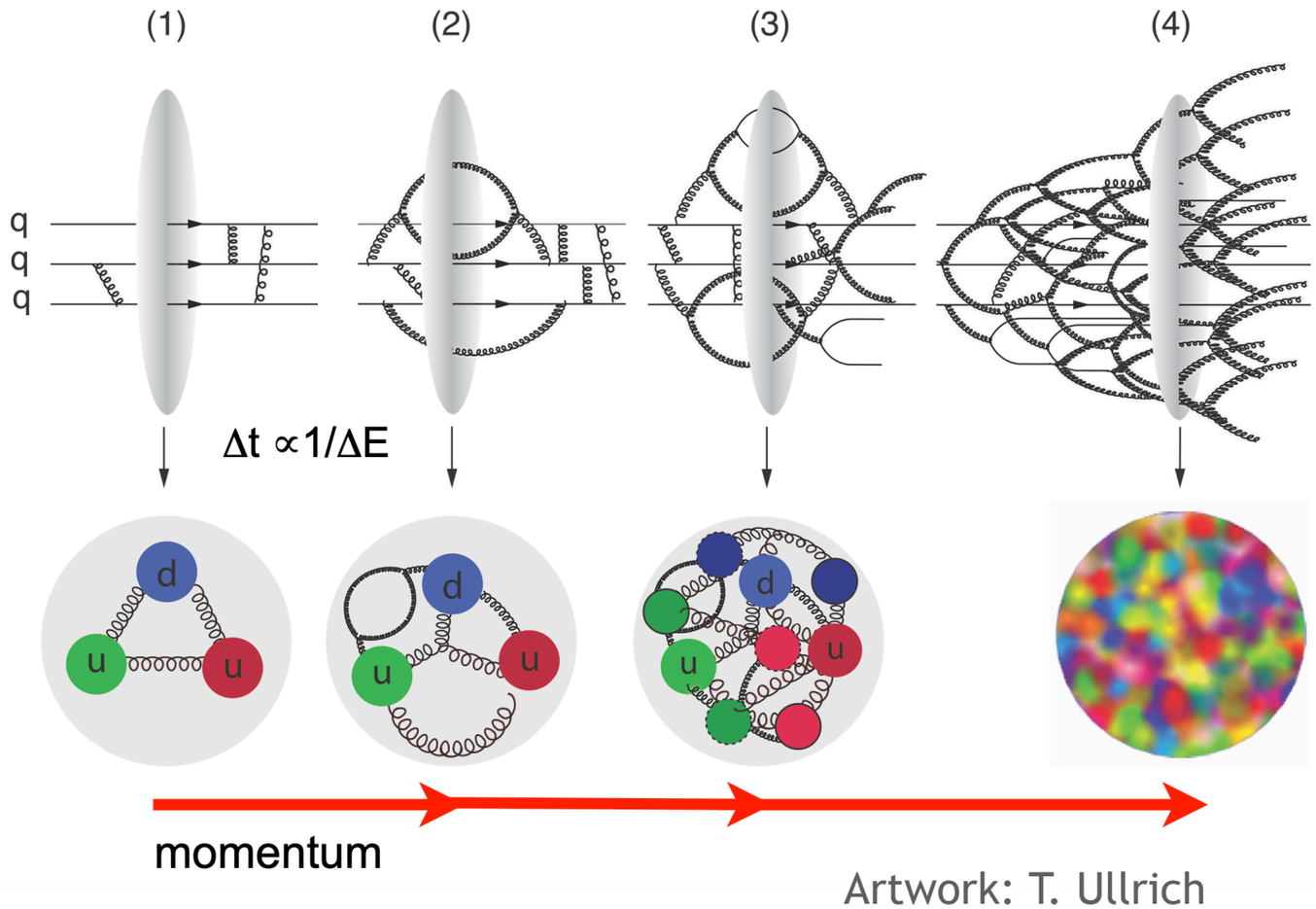

Artwork: T. Ullrich

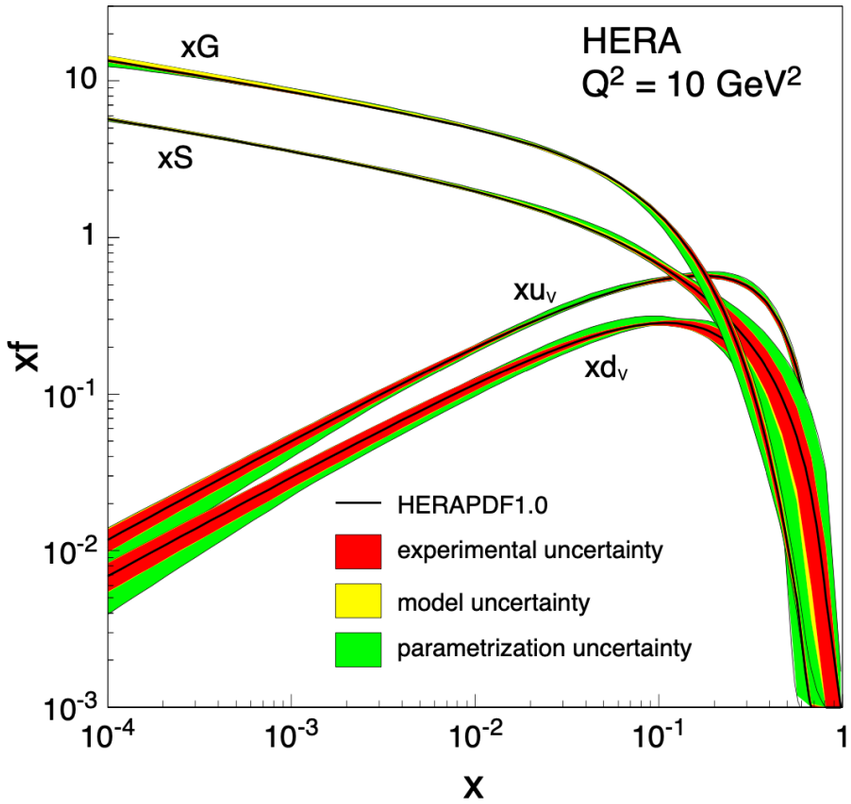

Emergence of an energy and nuclear specie dependent momentum scale (saturation scale)

Multiple scattering (higher twist effects)

Non-linear evolution equations (BK/JIMWLK)

$$Q_s^2 \propto A^{1/3} x^{-\lambda} \qquad x \propto 1/s$$

For a review see Mining gluon saturation at colliders. FS, Morreale (Universe 2021)

Quarkonium production in pp and pA

The Color Glass Condensate in a Nutshell: sources, field and Wilson lines

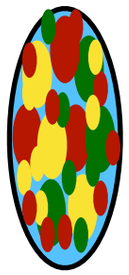

Large-x partons are effectively treated as a collection of recoilless localized and static random color sources

McLerran, Venugopalan (PRD 1993)

Source the back-ground field

$$A^+_{\rm cl}(\boldsymbol{x}_\perp, x^-) \sim 1/g$$

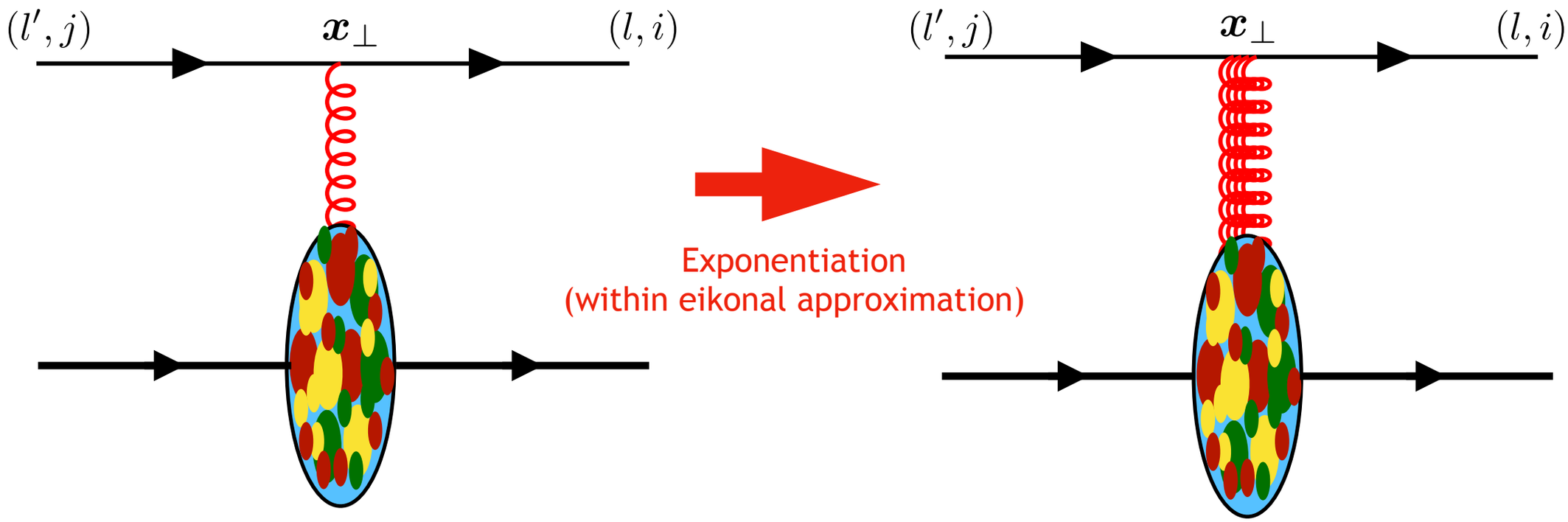

Exponentiation
(within eikonal approximation)

$$\mathcal{T}^q_{ij}(l, l') = (2\pi)\delta(l^- - l'^-)\gamma^- \mathrm{sgn}(l^-) \int_{\boldsymbol{x}_\perp} e^{-i(\boldsymbol{l}_\perp - \boldsymbol{l}'_\perp)\cdot \boldsymbol{z}_\perp} V_{ij}(\boldsymbol{x}_\perp)$$

Light-like Wilson line $$V_{ij}(\boldsymbol{x}_\perp) = P \exp\left\{ ig \int dx^- A^{+,a}_{\rm cl}(\boldsymbol{x}_\perp, x^-) t^a \right\}$$

Ayala, Jalilian-Marian, McLerran, Venugopalan (PRD 1995) Balistky (NPB 1996)

Quarkonium production in pp and pA

The Color Glass Condensate in a Nutshell: non-linear energy evolution

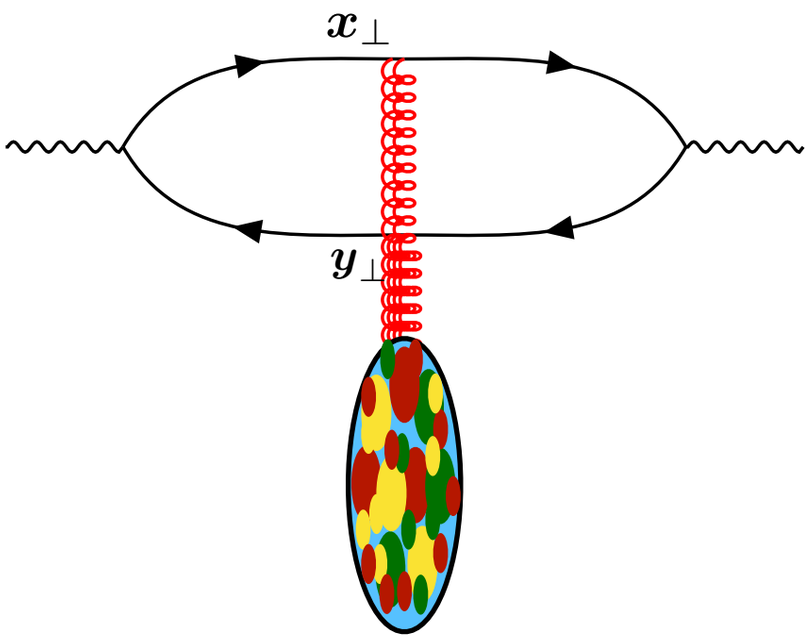

$$\mathrm{Tr}\left[V(\boldsymbol{x}_\perp)V^\dagger(\boldsymbol{y}_\perp)\right]$$

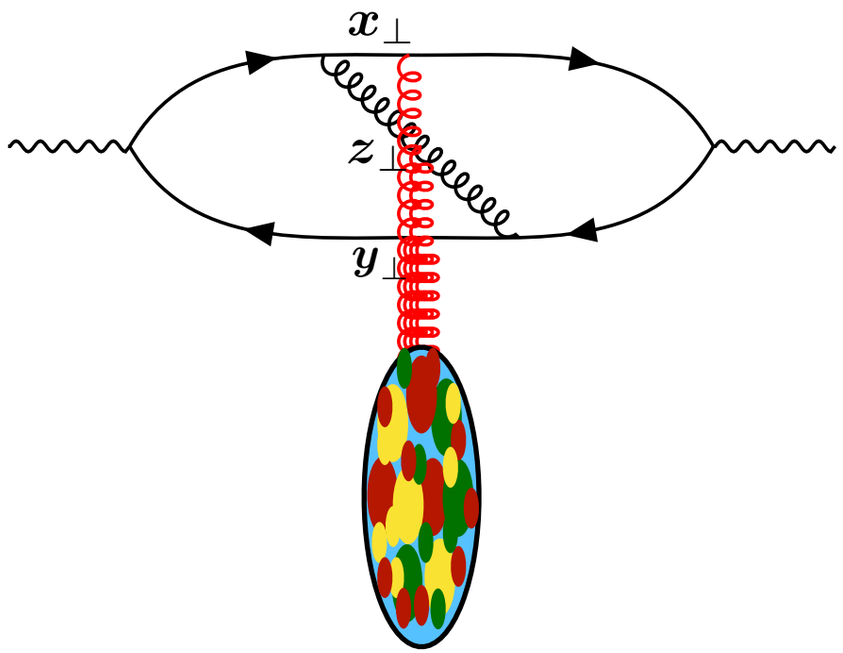

$$\mathrm{Tr}\left[V(\boldsymbol{x}_\perp)t^a V^\dagger(\boldsymbol{y}_\perp)t^b\right] U_{ab}(\boldsymbol{z}_\perp)$$

Dipole: $S^{(2)}(x;\boldsymbol{x}_\perp-\boldsymbol{y}_\perp)=\frac{1}{N_c}\left\langle \mathrm{Tr}\left[V(\boldsymbol{x}_\perp)V^\dagger(\boldsymbol{y}_\perp)\right]\right\rangle_x$

Gluon emissions lead to evolution (B-JIMWLK)

Balitsky-Kovchegov equation:

$$\frac{\mathrm{d}S^{(2)}(x;\boldsymbol{r}_\perp)}{\mathrm{d}\ln(1/x)}=\frac{\alpha_s N_c}{2\pi^2}\int \mathrm{d}^2\boldsymbol{r}'_\perp \frac{\boldsymbol{r}_\perp^2}{\boldsymbol{r}'^2_\perp(\boldsymbol{r}_\perp-\boldsymbol{r}'_\perp)^2}\left[S^{(2)}(x;\boldsymbol{r}'_\perp)S^{(2)}(x;\boldsymbol{r}_\perp-\boldsymbol{r}'_\perp)-S^{(2)}(x;\boldsymbol{r}_\perp)\right]$$

Balistky (NPB 1995), Kovchegov (PRD 1999)
Jalilian-Marian, Iancu, McLerran, Weigert, Leonidov, Kovner (1996-2002)

Quarkonium production in pp and pA

Charged hadron production

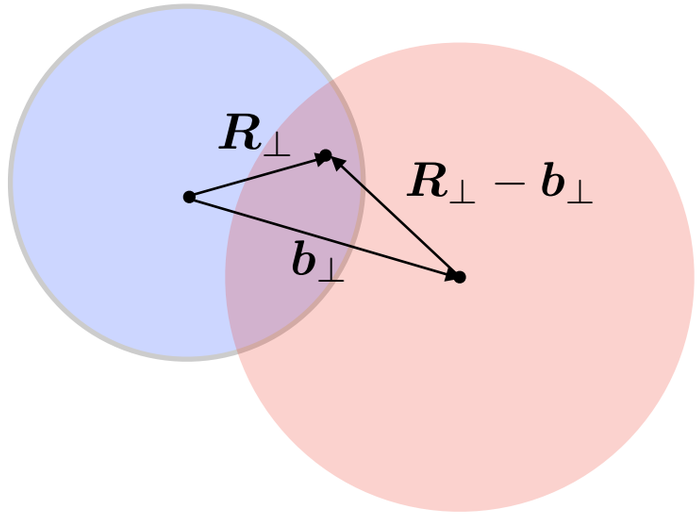

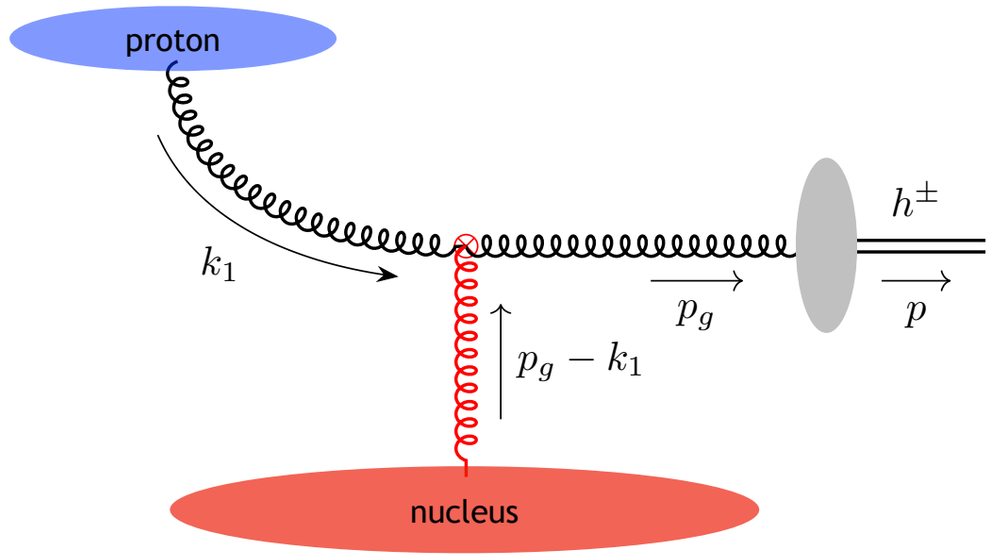

- k_T-factorization for gluon production

Kovchegov, Tuchin (PRD 2002)

$$\frac{\mathrm{d}N_g(\boldsymbol{b}_\perp)}{\mathrm{d}^2\boldsymbol{p_g}_\perp \mathrm{d}y_g} = \frac{\alpha_s}{(2\pi^2)^3 C_F} \frac{1}{\boldsymbol{p_g}_\perp^2} \int_{\boldsymbol{k_{1\perp}},\boldsymbol{k_{2\perp}},\boldsymbol{R}_\perp} \phi^p(x_p;\boldsymbol{k_{1\perp}};\boldsymbol{R}_\perp)\phi^A(x_A;\boldsymbol{k_{2\perp}};\boldsymbol{R}_\perp - \boldsymbol{b}_\perp)\delta^{(2)}(\boldsymbol{p_g}_\perp - \boldsymbol{k_{1\perp}} - \boldsymbol{k_{2\perp}})$$

- Unintegrated gluon distributions ϕ^p and ϕ^A constructed from Wilson lines with x-dependence from running coupling BK with MV initial conditions

- Hadronize using KKP fragmentation function

$$\frac{\mathrm{d}N_{\mathrm{ch}}(\boldsymbol{b}_\perp)}{\mathrm{d}\eta} = \int_{\boldsymbol{p}_\perp} \int_{z_{\min}}^1 \mathrm{d}z \frac{D_h(z)}{z^2} \mathcal{J}_{y\to\eta} \left.\frac{\mathrm{d}N_g(\boldsymbol{b}_\perp)}{\mathrm{d}^2\boldsymbol{p_g}_\perp \mathrm{d}y_g}\right|_{\boldsymbol{p_g}_\perp = \boldsymbol{p}_\perp/z}$$

Kniehl, Kramer, Pötter (NPB 2001)

Quarkonium production in pp and pA

J/ψ production in the Color Glass Condensate +ICEM

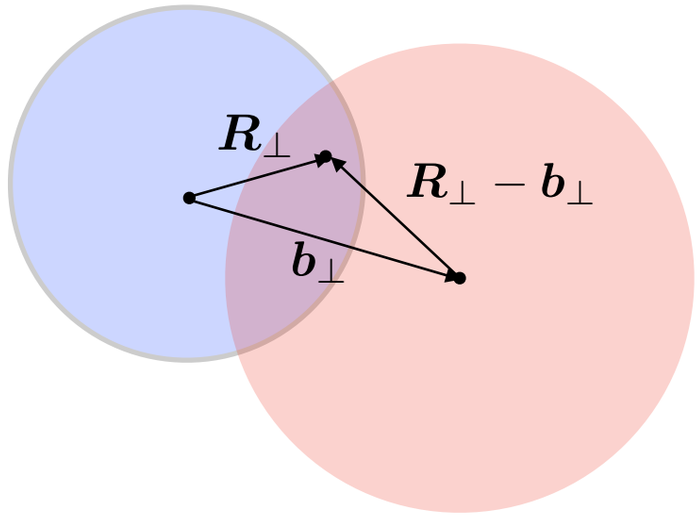

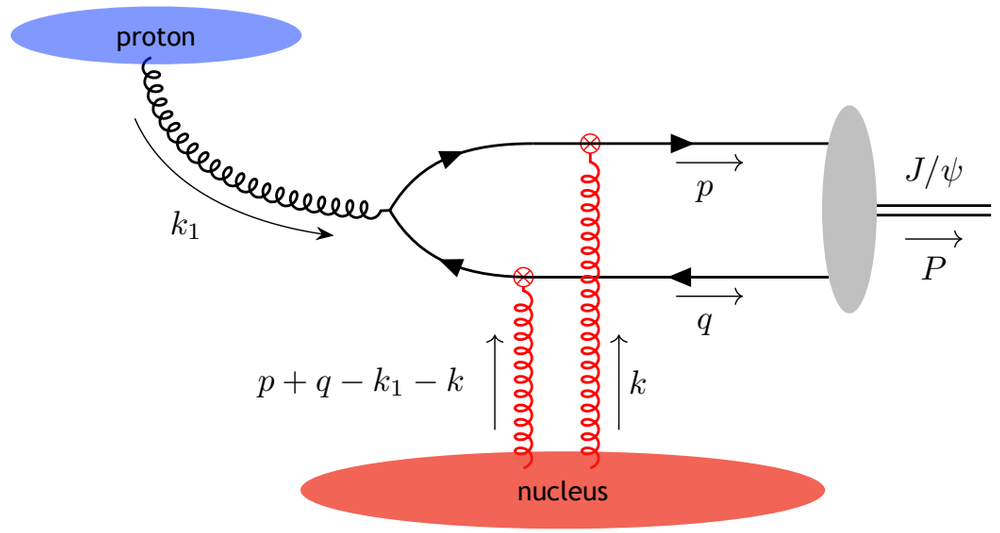

- $c\bar{c}$ production in the CGC (at large N_c)

Fujii, Gelis, Venugopalan (NPA 2006)

$$\frac{\mathrm{d}N_{c\bar{c}}(\boldsymbol{b}_\perp)}{\mathrm{d}^2\boldsymbol{p}_\perp \mathrm{d}^2\boldsymbol{q}_\perp \mathrm{d}y_c \mathrm{d}y_{\bar{c}}} = \frac{\alpha_s N_c^2}{2(2\pi)^{10}(N_c^2-1)} \int_{\boldsymbol{k_{1\perp}},\boldsymbol{k}_\perp,\boldsymbol{l}_\perp,\boldsymbol{R}_\perp} \frac{\phi^p(x_p;\boldsymbol{k_{1\perp}};\boldsymbol{R}_\perp)}{\boldsymbol{k_{1\perp}}^2} \widetilde{\mathcal{S}}^A_{\mathrm{F}}(x_A;\boldsymbol{k}_\perp;\boldsymbol{R}_\perp-\boldsymbol{b}_\perp)\widetilde{\mathcal{S}}^A_{\mathrm{F}}(x_A;\boldsymbol{l}_\perp;\boldsymbol{R}_\perp-\boldsymbol{b}_\perp)$$
$$\mathcal{H}(\boldsymbol{p}_\perp,\boldsymbol{q}_\perp;\boldsymbol{k_{1\perp}},\boldsymbol{k}_\perp,\boldsymbol{l}_\perp)\ \delta^{(2)}(\boldsymbol{p}_\perp+\boldsymbol{q}_\perp-\boldsymbol{k_{1\perp}}-\boldsymbol{k}_\perp-\boldsymbol{l}_\perp)$$

- Scattering of quarks contained in $\widetilde{S}^A_{\mathrm{F}}$ constructed from Wilson lines with x-dependence from running coupling BK with MV initial conditions

- Formation of J/ψ using Improved Color Evaporation Model

Ma, Vogt (PRD 2016)

$$\frac{\mathrm{d}N_{J/\psi}(\boldsymbol{b}_\perp)}{\mathrm{d}^2\boldsymbol{P}_\perp \mathrm{d}Y} = F \int_{m^2_{J/\psi}}^{4m^2_D} \mathrm{d}M^2 \frac{M^2}{m^2_{J/\psi}} \frac{\mathrm{d}N_{c\bar{c}}(\boldsymbol{b}_\perp)}{\mathrm{d}M^2 \mathrm{d}^2\boldsymbol{P}'_\perp \mathrm{d}Y}\bigg|_{\boldsymbol{P}'_\perp = \frac{M}{m_{J/\psi}}\boldsymbol{P}_\perp}$$

Quarkonium production in pp and pA

J/ψ production in the Color Glass Condensate + NRQCD

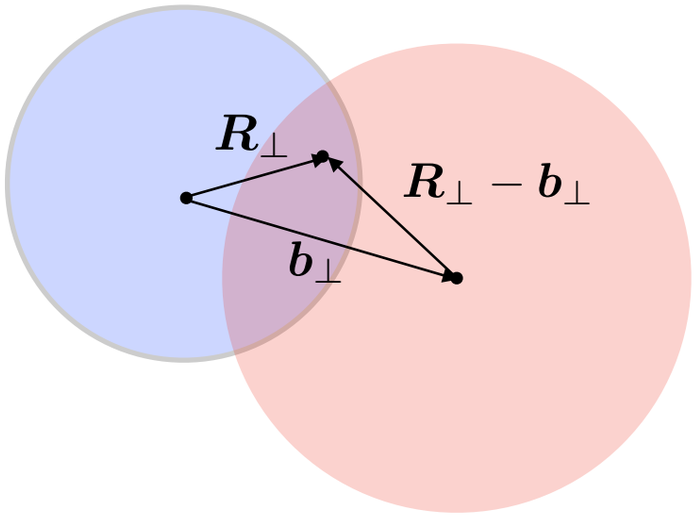

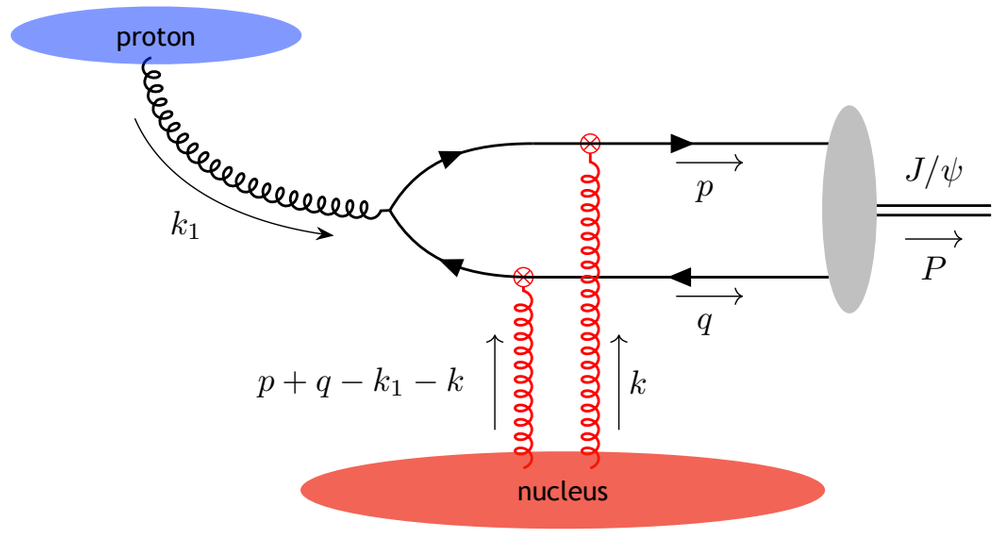

- NRQCD: product of short-distance coefficient with long-distance matrix elements

$$\frac{\mathrm{d}N_{J/\psi}(\boldsymbol{b}_\perp)}{\mathrm{d}^2\boldsymbol{P}_\perp \mathrm{d}Y} = \sum_\kappa \frac{\mathrm{d}N^\kappa_{c\bar{c}}(\boldsymbol{b}_\perp)}{\mathrm{d}^2\boldsymbol{P}_\perp \mathrm{d}Y} \langle \mathcal{O}^{J/\psi}_\kappa \rangle$$

- Short-distance coefficients, $c\bar{c}$ projected to a given quantum state $\kappa = {}^{2S+1}L^{[C]}_J$)

$$\frac{\mathrm{d}N^\kappa_{c\bar{c}}(\boldsymbol{b}_\perp)}{\mathrm{d}^2\boldsymbol{P}_\perp \mathrm{d}Y} = \frac{\alpha_s}{(2\pi)^9 (N_c^2-1)} \int_{\boldsymbol{k_{1\perp}},\boldsymbol{k}_\perp,\boldsymbol{k}'_\perp,\boldsymbol{l}_\perp,\boldsymbol{R}_\perp} \frac{\phi^p(x_p,\boldsymbol{k_{1\perp}},\boldsymbol{R}_\perp)}{\boldsymbol{k_{1\perp}}^2} \widetilde{\Xi}^\kappa(x_A;\boldsymbol{k}_\perp,\boldsymbol{k}'_\perp,\boldsymbol{l}_\perp;\boldsymbol{R}_\perp-\boldsymbol{b}_\perp)$$
$$\mathcal{H}^\kappa(\boldsymbol{P}_\perp;\boldsymbol{k_{1\perp}},\boldsymbol{k}_\perp,\boldsymbol{l}_\perp,\boldsymbol{k}'_\perp)\, \delta^{(2)}(\boldsymbol{p}_\perp+\boldsymbol{q}_\perp-\boldsymbol{k_{1\perp}}-\boldsymbol{k}_\perp-\boldsymbol{l}_\perp)$$

Kang, Ma, Venugopalan (JHEP 2014)

- $\widetilde{\Xi}^\kappa$ color correlator and $\mathcal{H}^\kappa$ depend on quantum state κ

Quarkonium production in pp and pA

Transverse momentum distribution

Proton-proton at RHIC and LHC

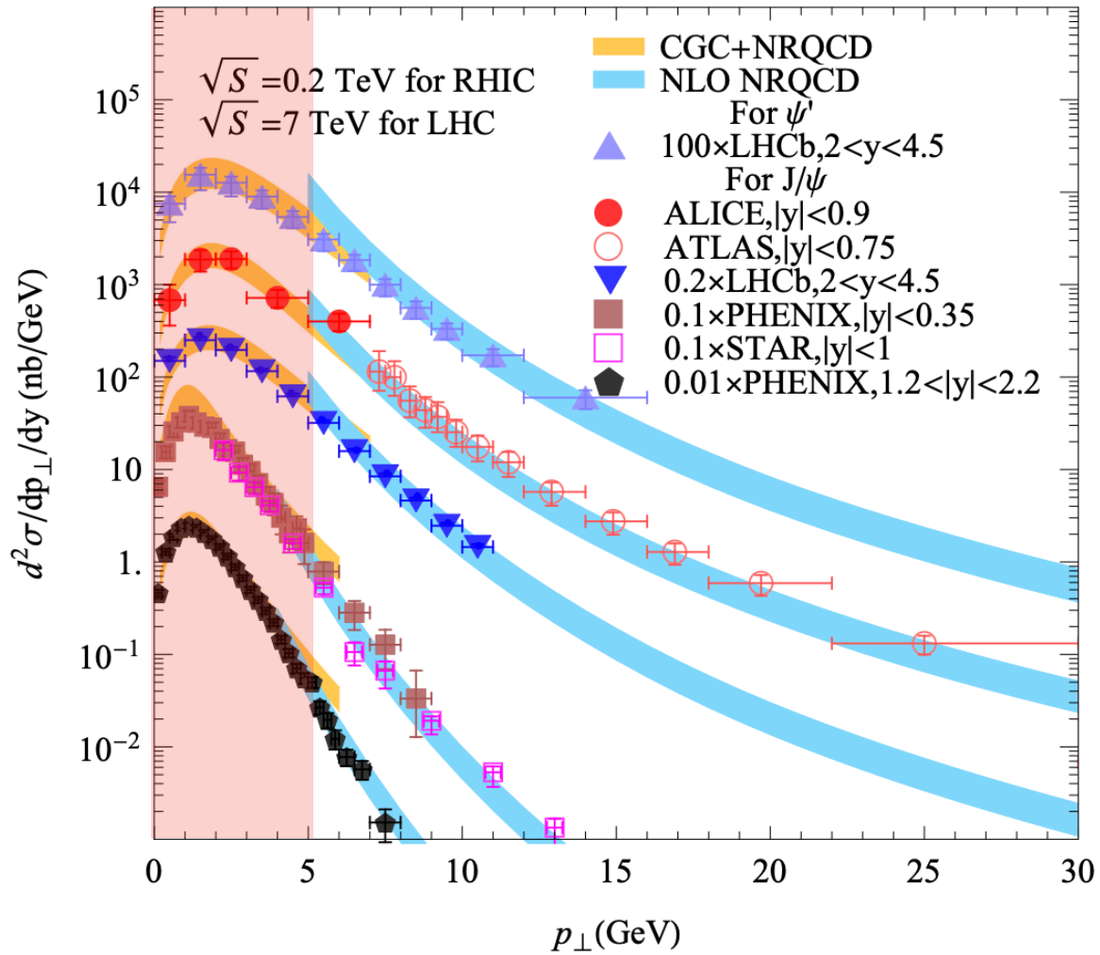

Ma, Venugopalan (PRL 2014)

Proton-nucleus at RHIC and LHC

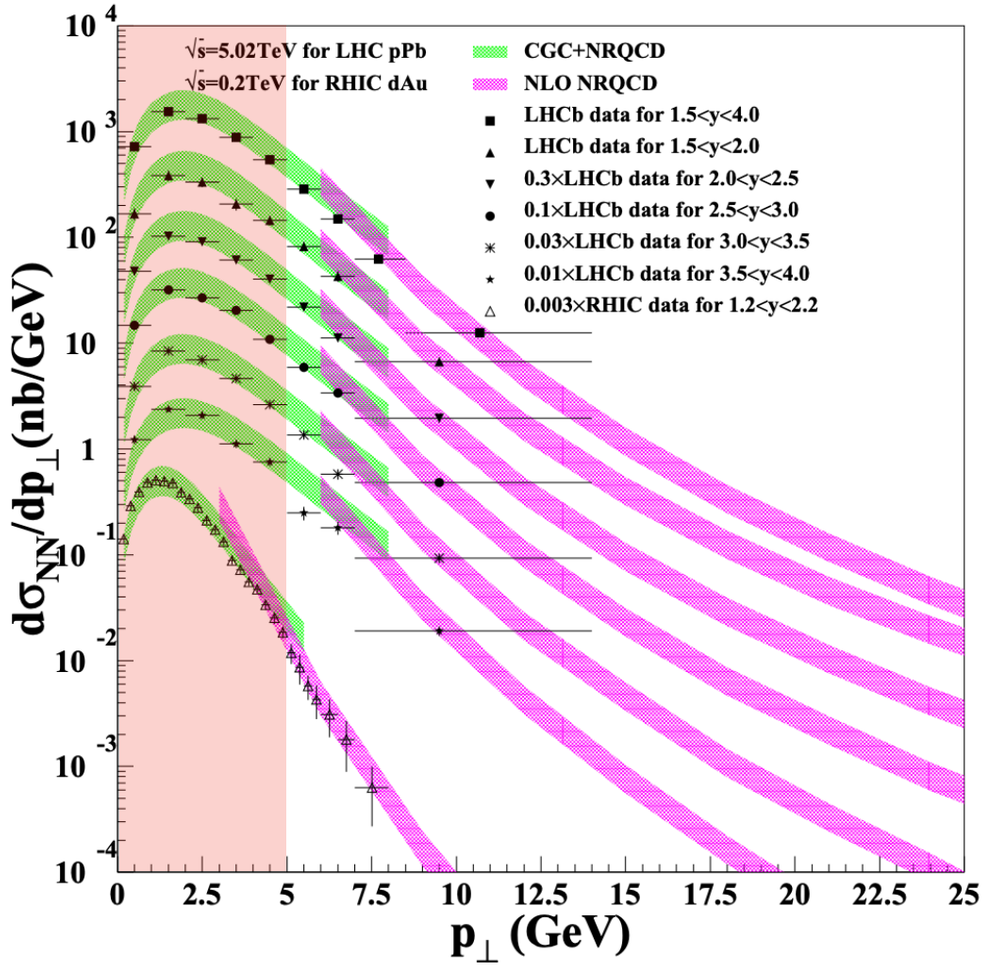

Ma, Venugopalan, Zhang (PRD 2015)

CGC provides good description of experimental data at low pT ($p_\perp \lesssim Q_s$)

For bottonia need to resum additional Sudakov logs in $p_\perp/M$, see Watanabe, Xiao (PRD 2015)

Quarkonium production in pp and pA

Rapidity distribution

Proton-proton at LHC

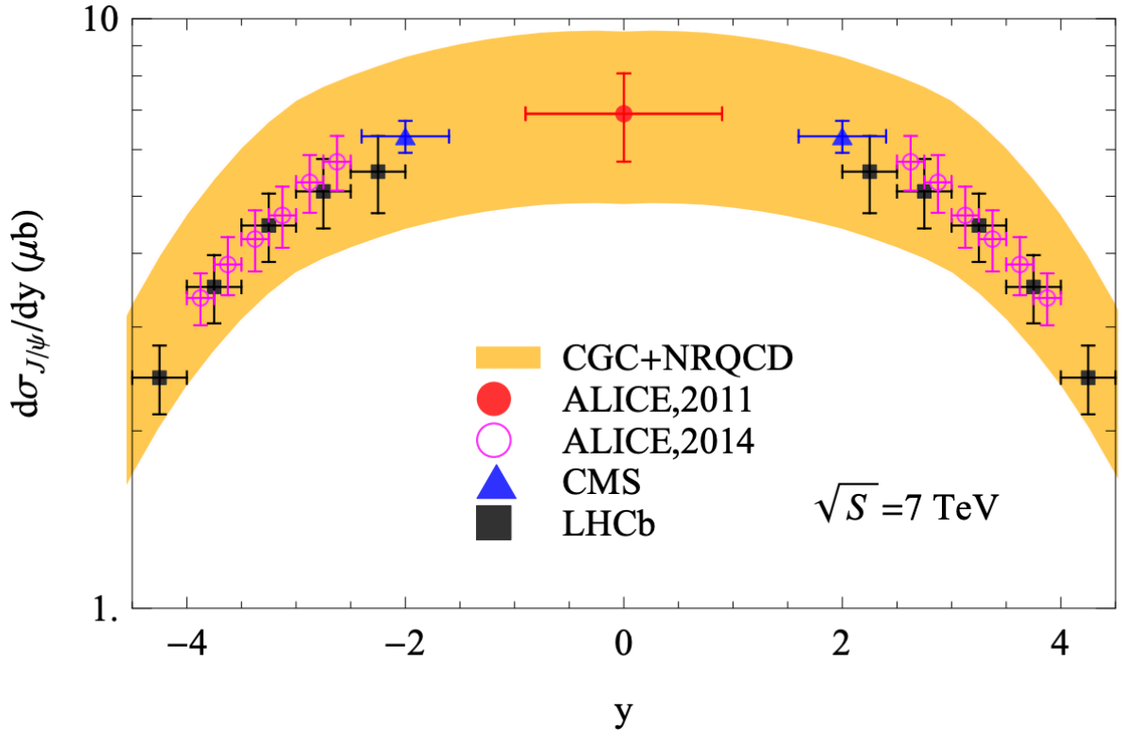

Ma, Venugopalan (PRL 2014)

Proton-nucleus at LHC

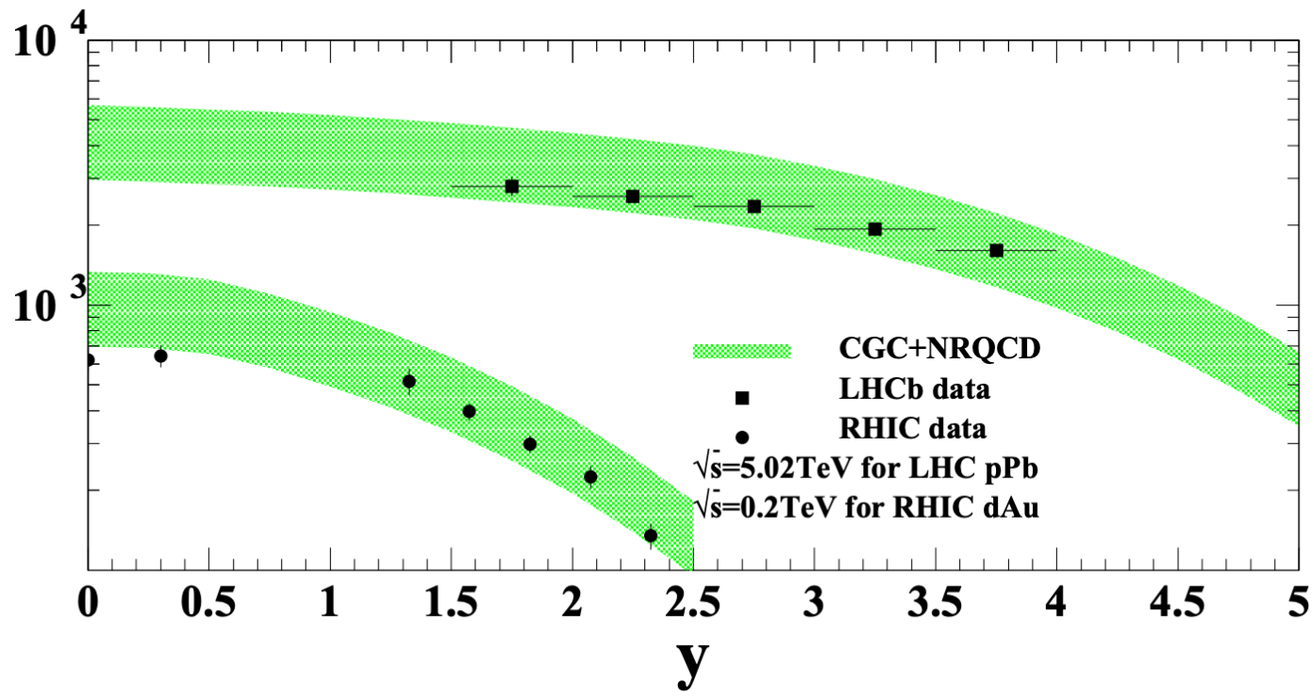

Ma, Venugopalan, Zhang (PRD 2015)

Forward production $Y \gg 1 \longrightarrow x_p \sim 1, x_A \ll 1$

Backward production $Y \ll -1 \longrightarrow x_p \ll 1, x_A \sim 1$

- Matching to PDFs is implemented for $x \gtrsim 0.01$
- Distributions integrated over $p_\perp$ (low $p_\perp$ region dominates so CGC at leading order should be applicable)

CGC provides good description across different rapidities

Quarkonium production in pp and pA

Nuclear modification ratio

Ma, Venugopalan, Zhang (PRD 2015)

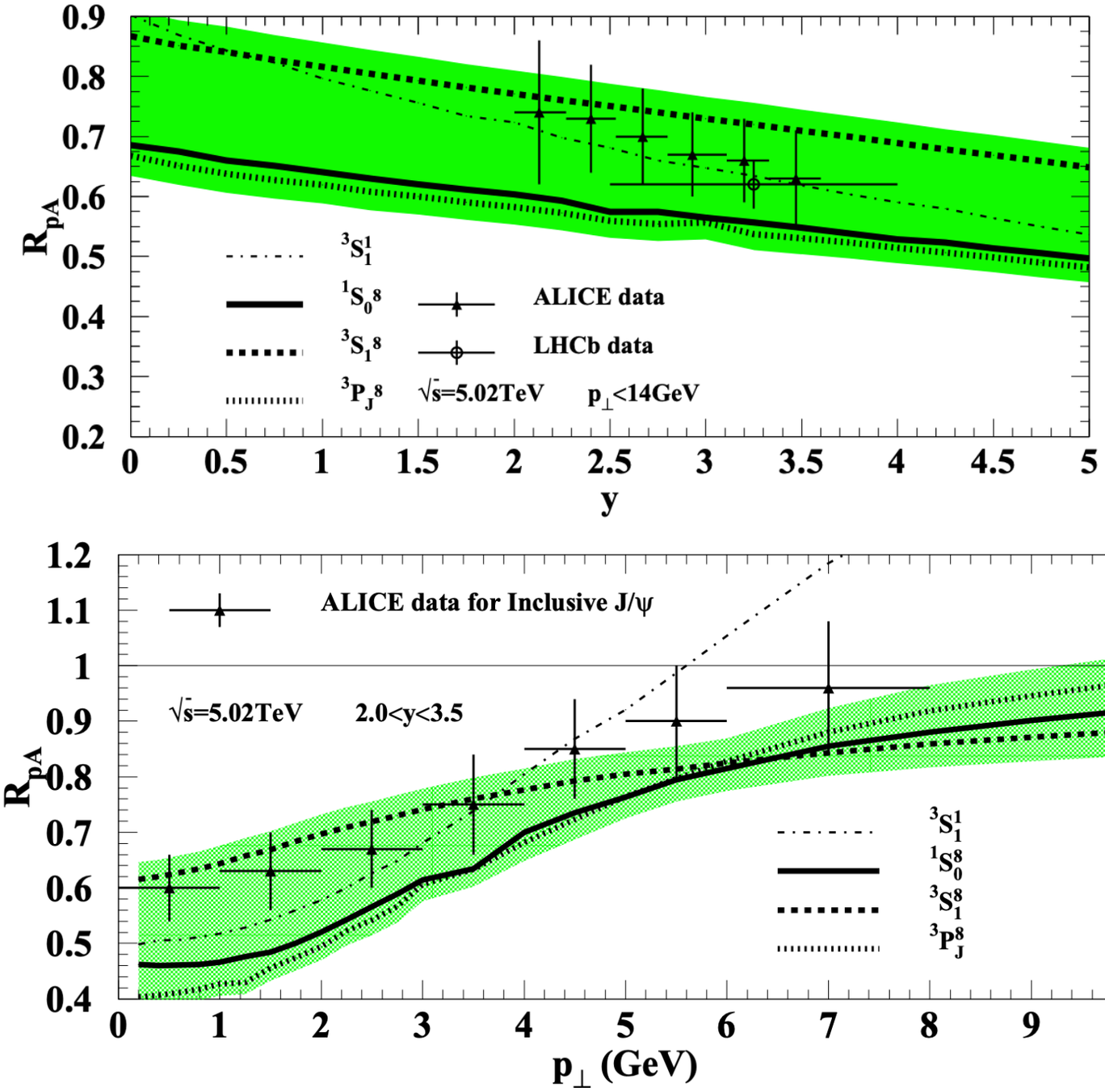

Nuclear modification ratio in CGC + NRQCD

Quarkonium production in pp and pA

J/ψ multiplicity vs charged hadron multiplicity

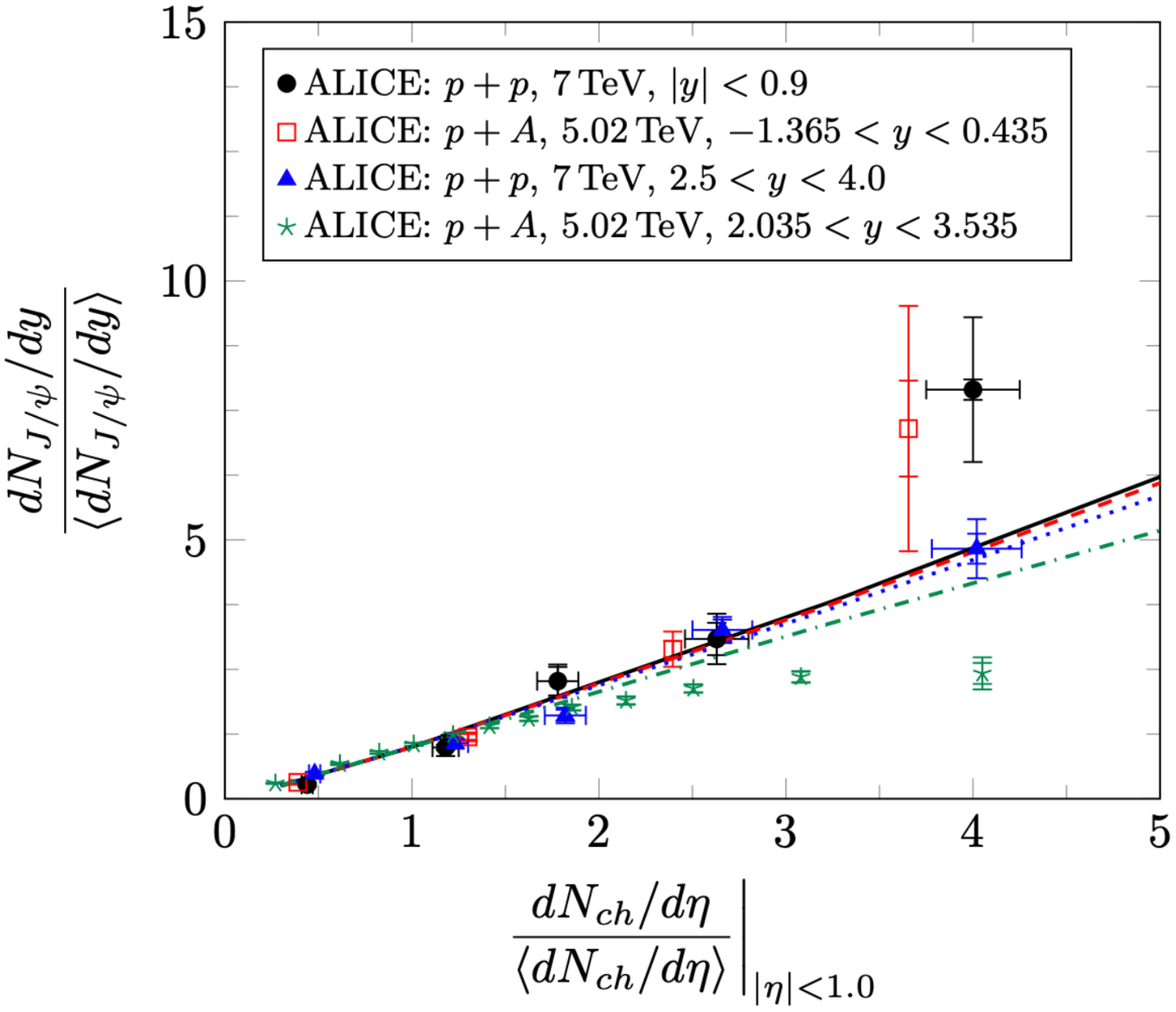

Ma, Stebel, Venugopalan, Watanabe (Hard Probes 2020)

See also Ma, Tribedy, Venugopalan, Watanabe (PRD 2018)

In the CGC multiplicity is controlled by the saturation scales of the proton and nucleus: Q_{sp}^2 and Q_{sA}^2

Minimum-bias events

$$\left\langle \frac{\mathrm{d}N_{ch}^{pA}}{\mathrm{d}\eta} \right\rangle \equiv \left. \frac{\mathrm{d}N_{ch}}{\mathrm{d}\eta} \right|_{\substack{Q_{sp,\mathrm{M.B.}}^2 \\ Q_{sA,\mathrm{M.B.}}^2}}$$

Different multiplicity classes: introduce multiplicative parameter ξ

$$\frac{\mathrm{d}N_{ch}^{pA}}{\mathrm{d}\eta} \equiv \left. \frac{\mathrm{d}N_{ch}}{\mathrm{d}\eta} \right|_{\substack{\xi Q_{sp,\mathrm{M.B.}}^2 \\ \xi Q_{sA,\mathrm{M.B.}}^2}}$$

Low-multiplicity: $0 < \xi < 1$

High-multiplicity: $\xi > 1$

Sub-nuclear fluctuations

Fluctuating nucleons, hotspots, and saturation

Previous works ignored impact parameter dependence, i.e. partons are homogeneously distributed in transverse space

- Sample impact parameter vector $\boldsymbol{b}_\perp$ of collision

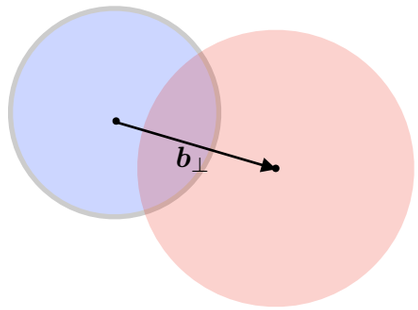

- Sample nucleon position from Woods-Saxon distribution

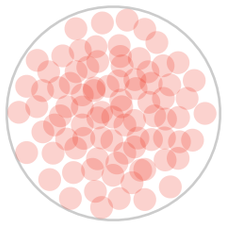

- Each nucleon consists of 3 hotspots sampled from a Gaussian distribution

$$P(\boldsymbol{R}_{\perp i}) = \frac{1}{2\pi B_{\mathrm{qc}}} e^{-\boldsymbol{R}_{\perp i}^2/(2B_{qc})}$$

Mäntysaari, Schenke (PRL 2015)

- Hotspots gluon density distribution

$$T_q(\boldsymbol{R}_\perp - \boldsymbol{R}_{\perp,i}) = \xi_{Q_s^2} e^{-(\boldsymbol{R}_\perp - \boldsymbol{R}_{\perp,i})^2/(2(\xi_{B_q})B_q)}$$

fluctuating normalization — fluctuating size

- ξ_{Qs^2} and ξ_{B_q} sampled from log-normal distribution

$$P(\ln p_i) = \frac{1}{\sqrt{2\pi}\sigma} \exp\left[-\frac{\ln^2 p_i}{2\sigma^2}\right]$$

Sub-nuclear fluctuations

Transverse momentum and rapidity distributions

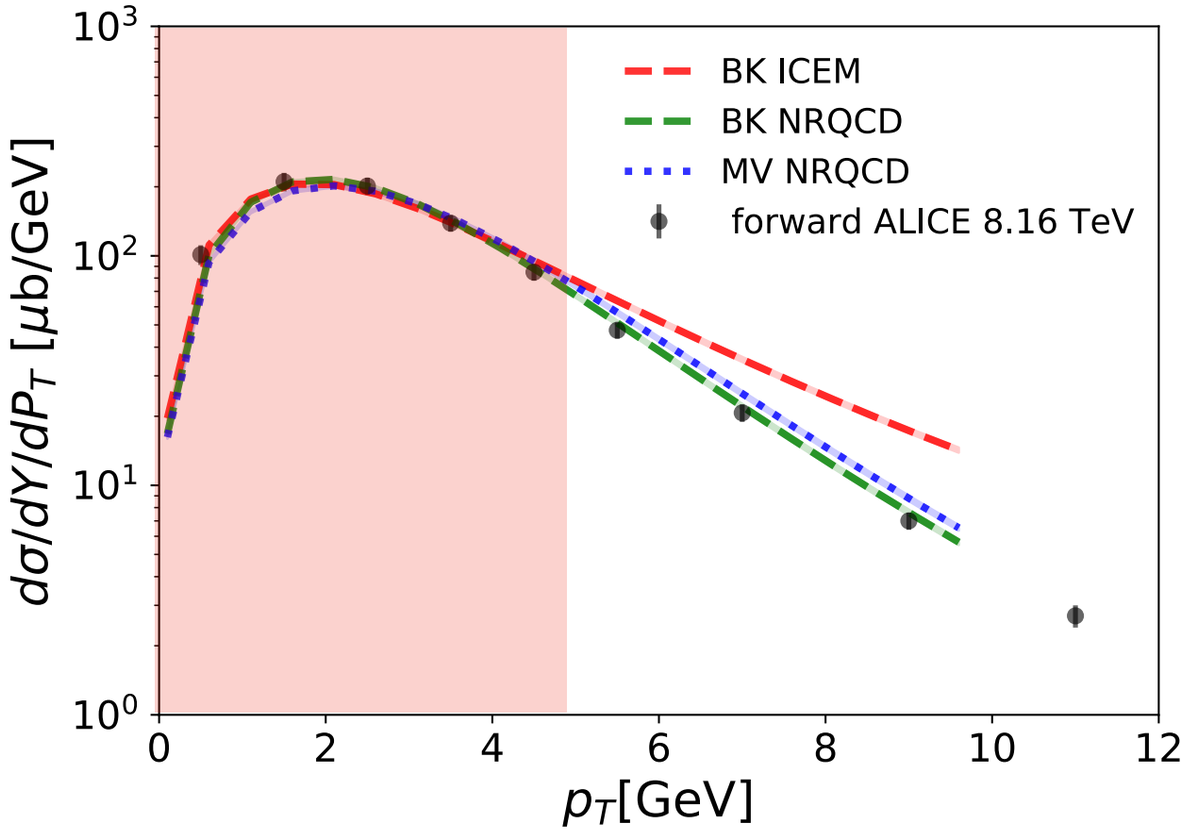

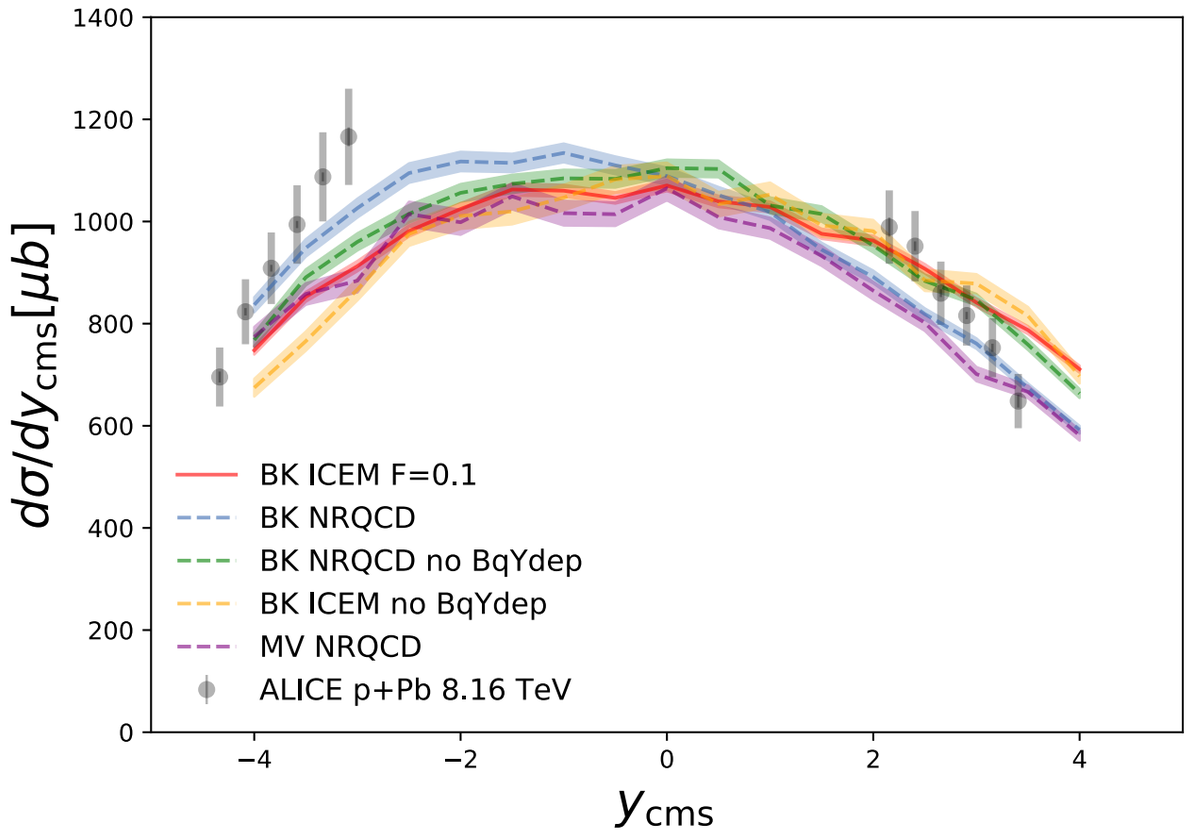

Experimental data: S. Acharya et al. (ALICE, JHEP 2020)

Theory results include sub-nuclear fluctuations

Good description of experimental data at low pT ($p_\perp \lesssim 5$ GeV), and reasonable description of rapidity distribution (both forward and backward)

FS, Schenke, Soto-Ontoso work in progress

Sub-nuclear fluctuations

Nuclear modification ratio

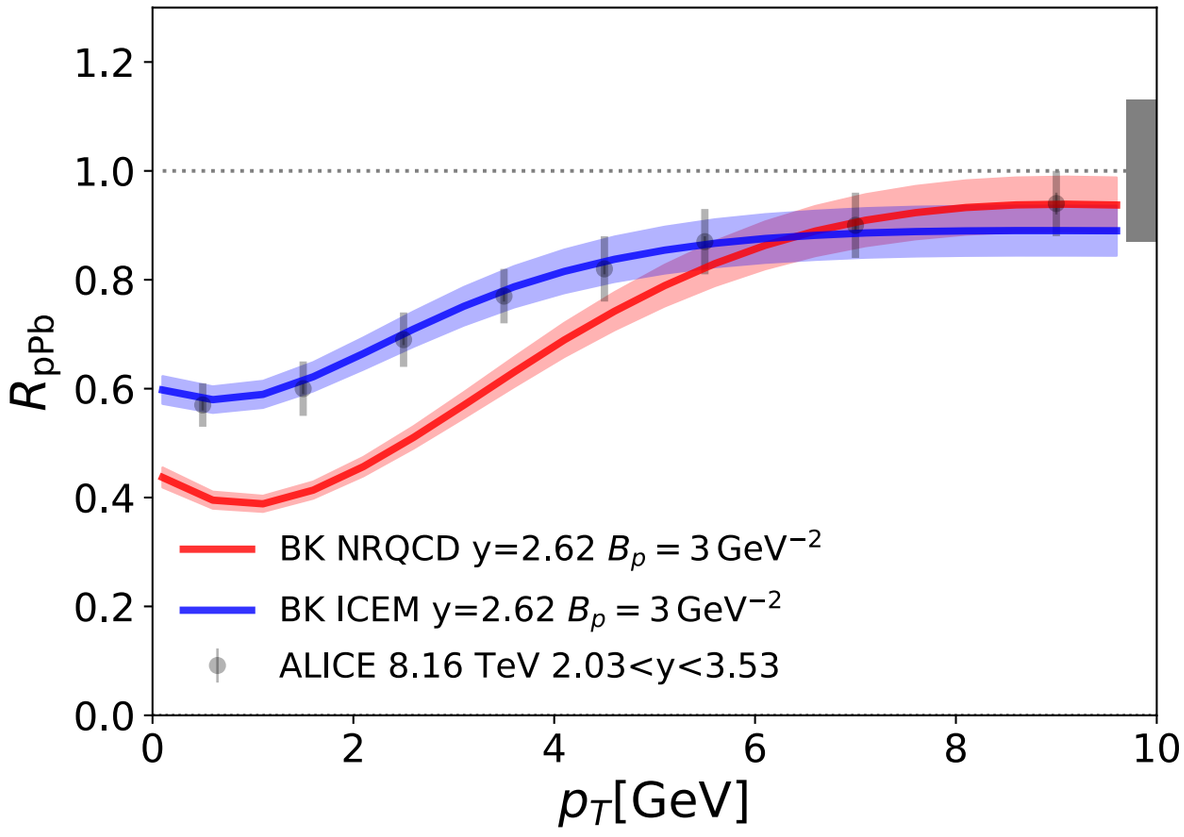

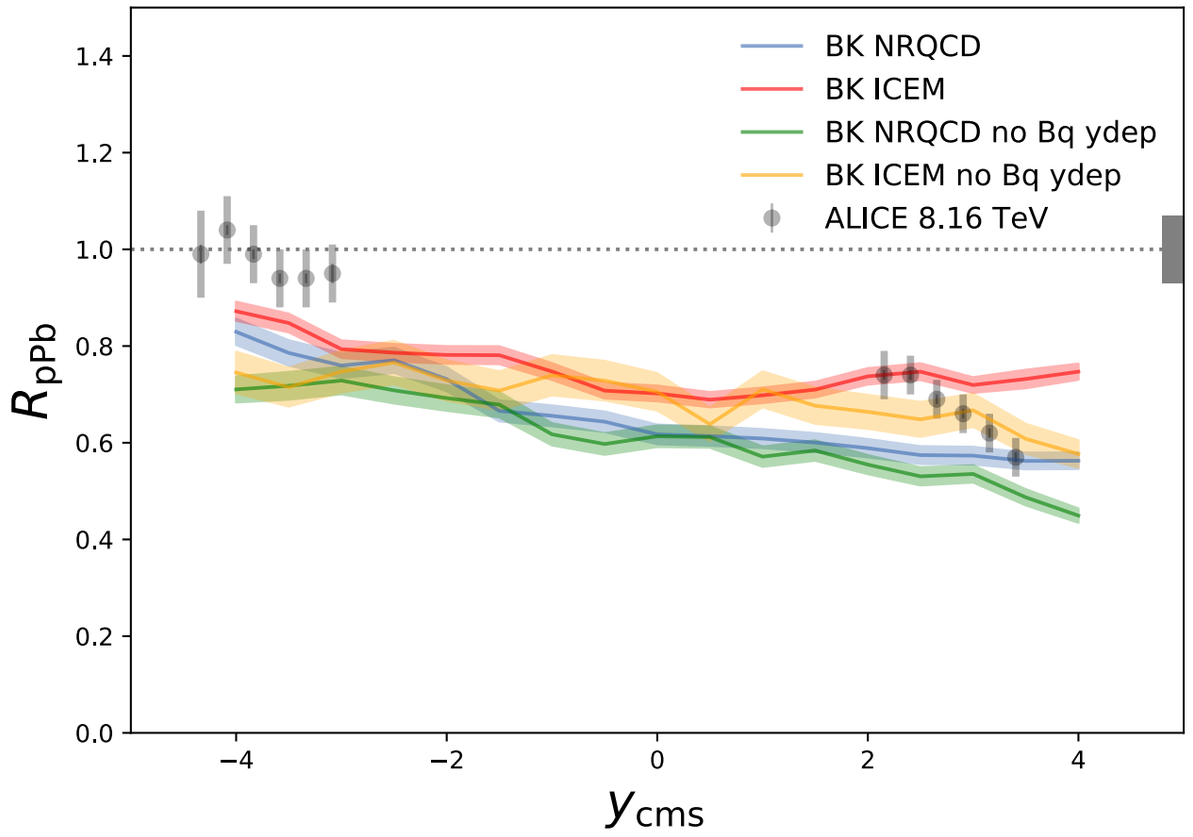

Experimental data: S. Acharya et al. (ALICE, JHEP 2020)

Theory results include sub-nuclear fluctuations

Overall NRQCD results in more nuclear suppression than ICEM due to different state projections in the former

FS, Schenke, Soto-Ontoso work in progress

Sub-nuclear fluctuations

J/ψ multiplicity vs charged hadron multiplicity: saturation

FS, Schenke, Soto-Ontoso *[PLB 827 (2022) 136952]*

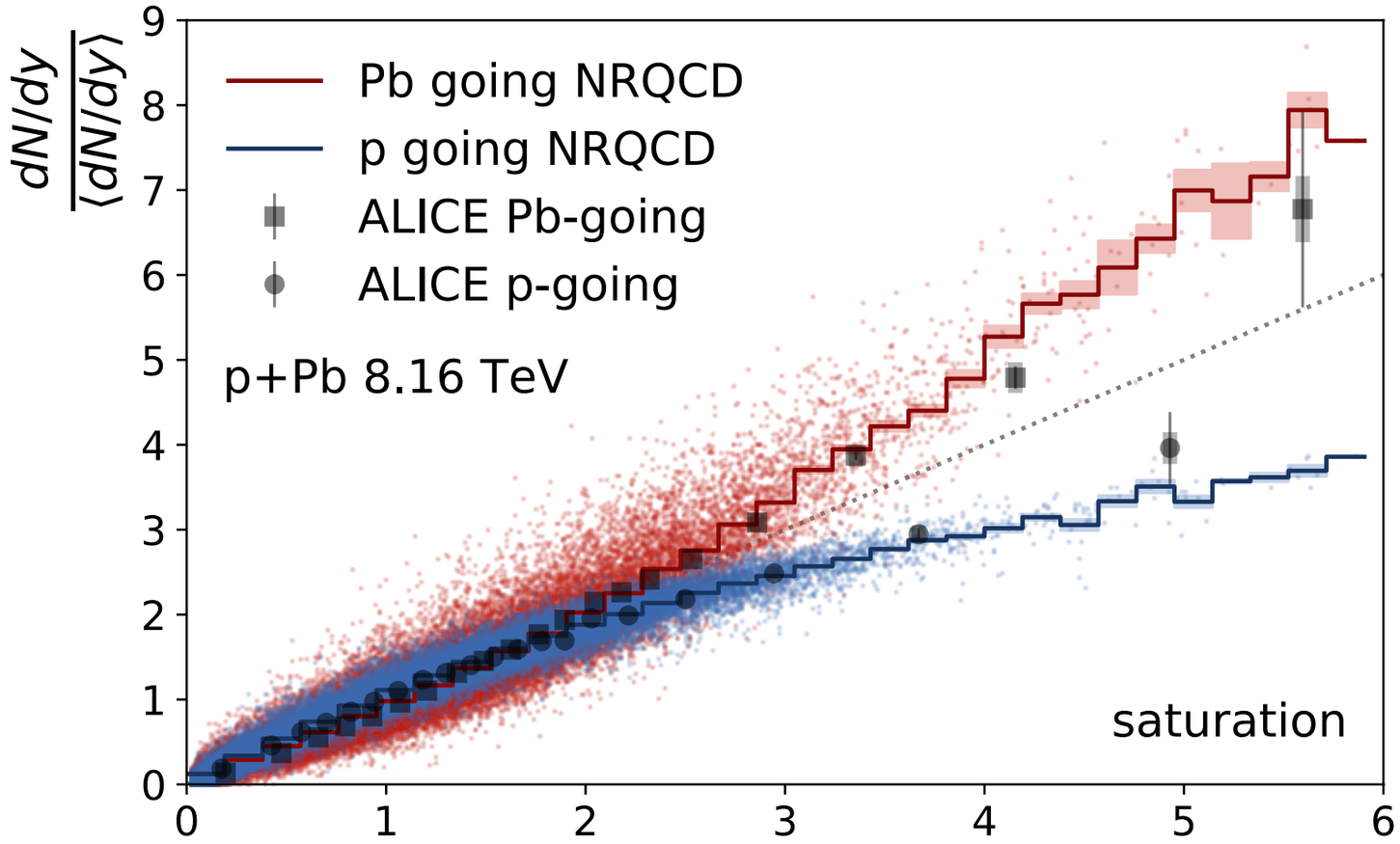

Experimental data: S. Acharya et al. (ALICE, JHEP 2020)

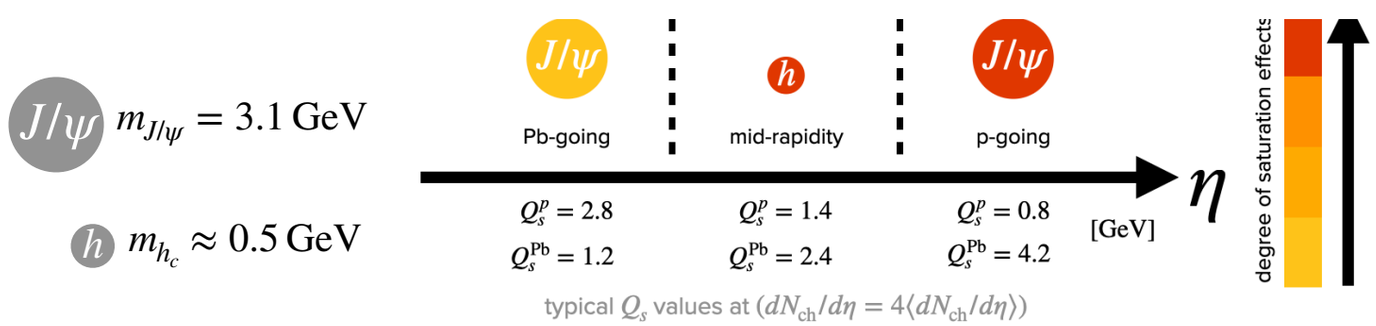

Sub-nuclear fluctuations

J/ψ multiplicity vs charged hadron multiplicity: no saturation

FS, Schenke, Soto-Ontoso *[PLB 827 (2022) 136952]*

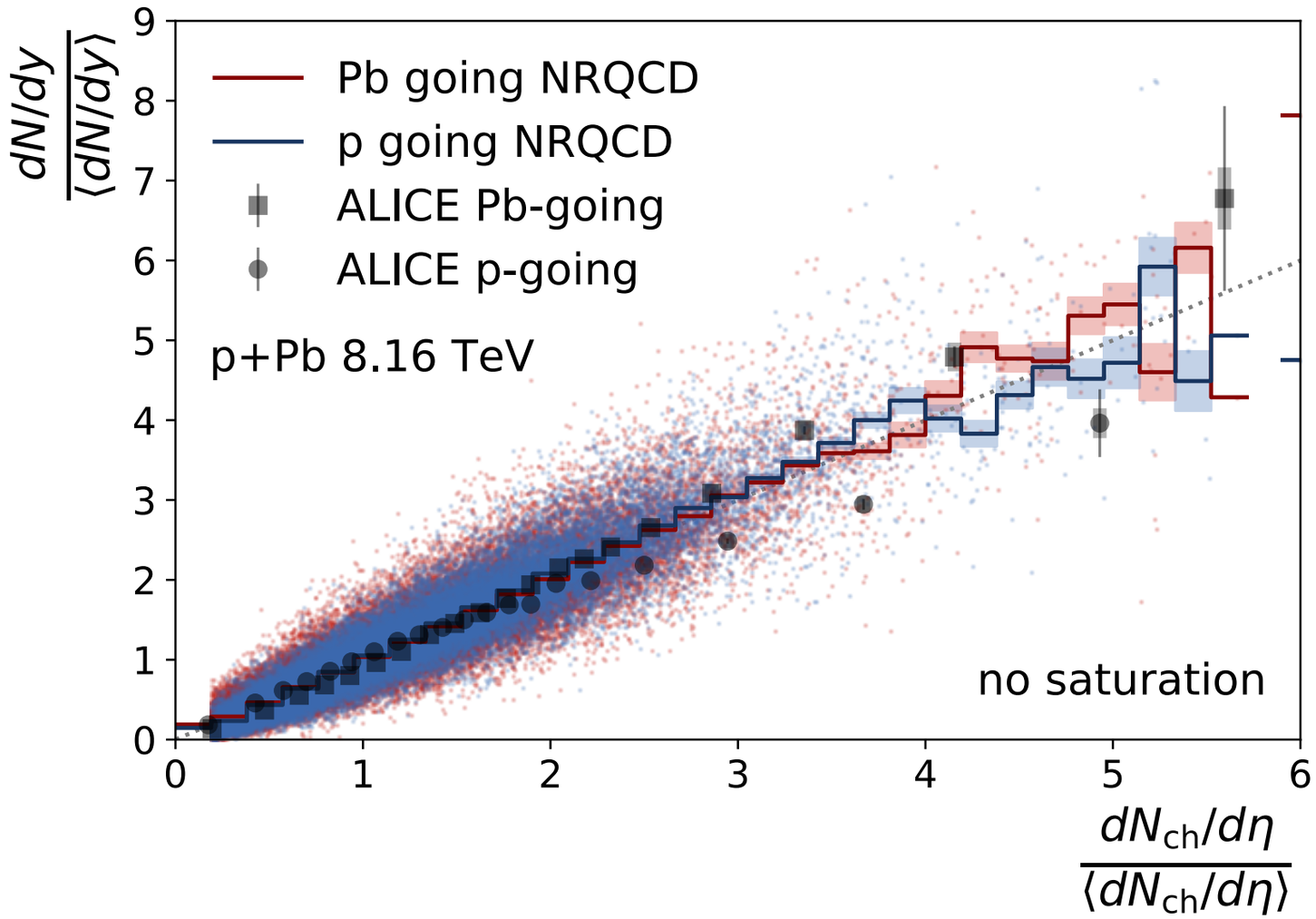

Artificially low values of Q_s to mimic of no, or much weaker, saturation effects.
Correlator is much closer to the diagonal incompatible with the data.

Sub-nuclear fluctuations

J/ψ multiplicity vs charged hadron multiplicity: no size fluctuations

FS, Schenke, Soto-Ontoso *[PLB 827 (2022) 136952]*

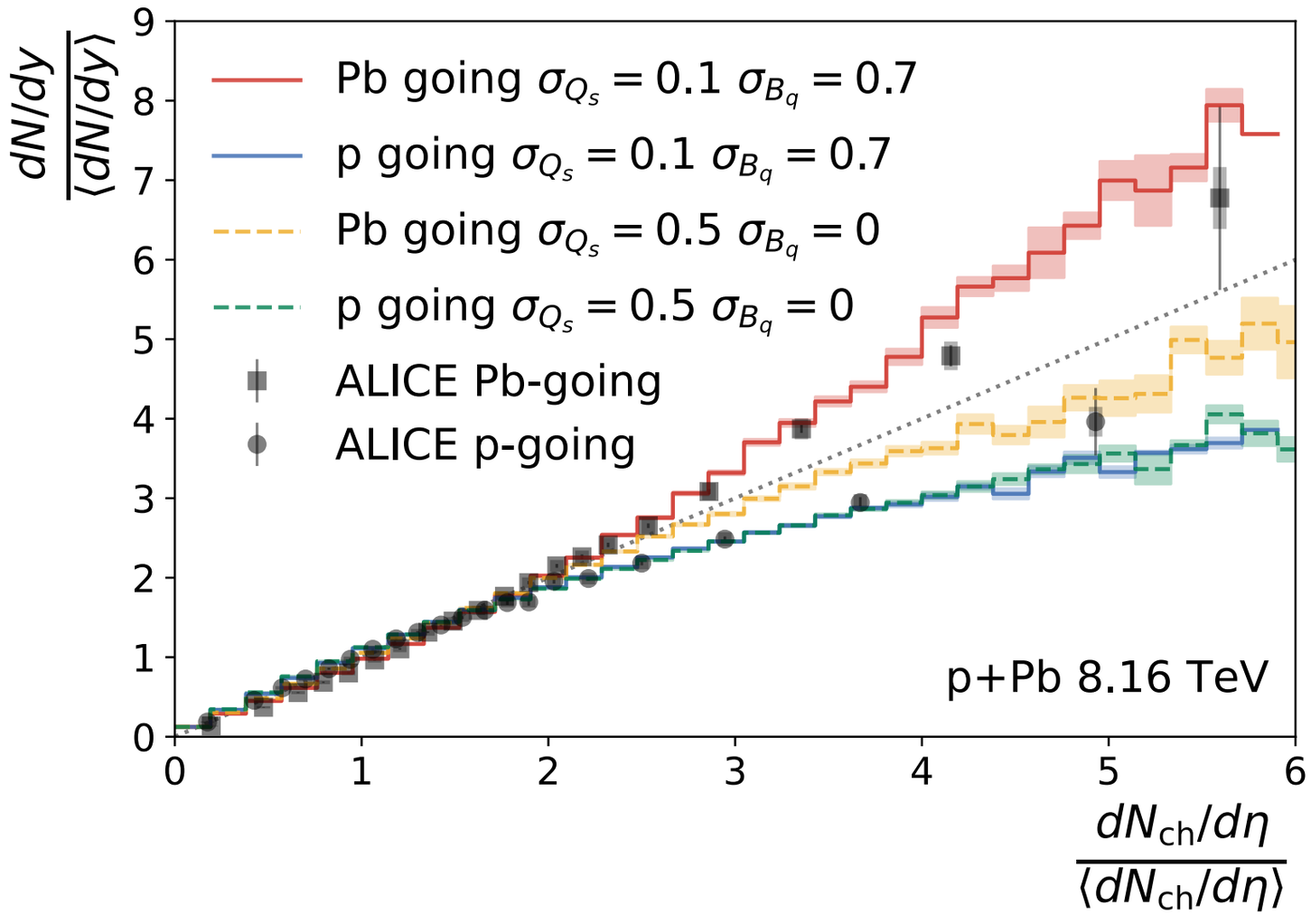

When turning off hotspot size fluctuations, high multiplicity events are reached only by large fluctuations of the saturation scale, thus too strong saturation effects.

Sub-nuclear fluctuations

J/ψ multiplicity vs charged hadron multiplicity: NRQCD vs ICEM

FS, Schenke, Soto-Ontoso *[PLB 827 (2022) 136952]*

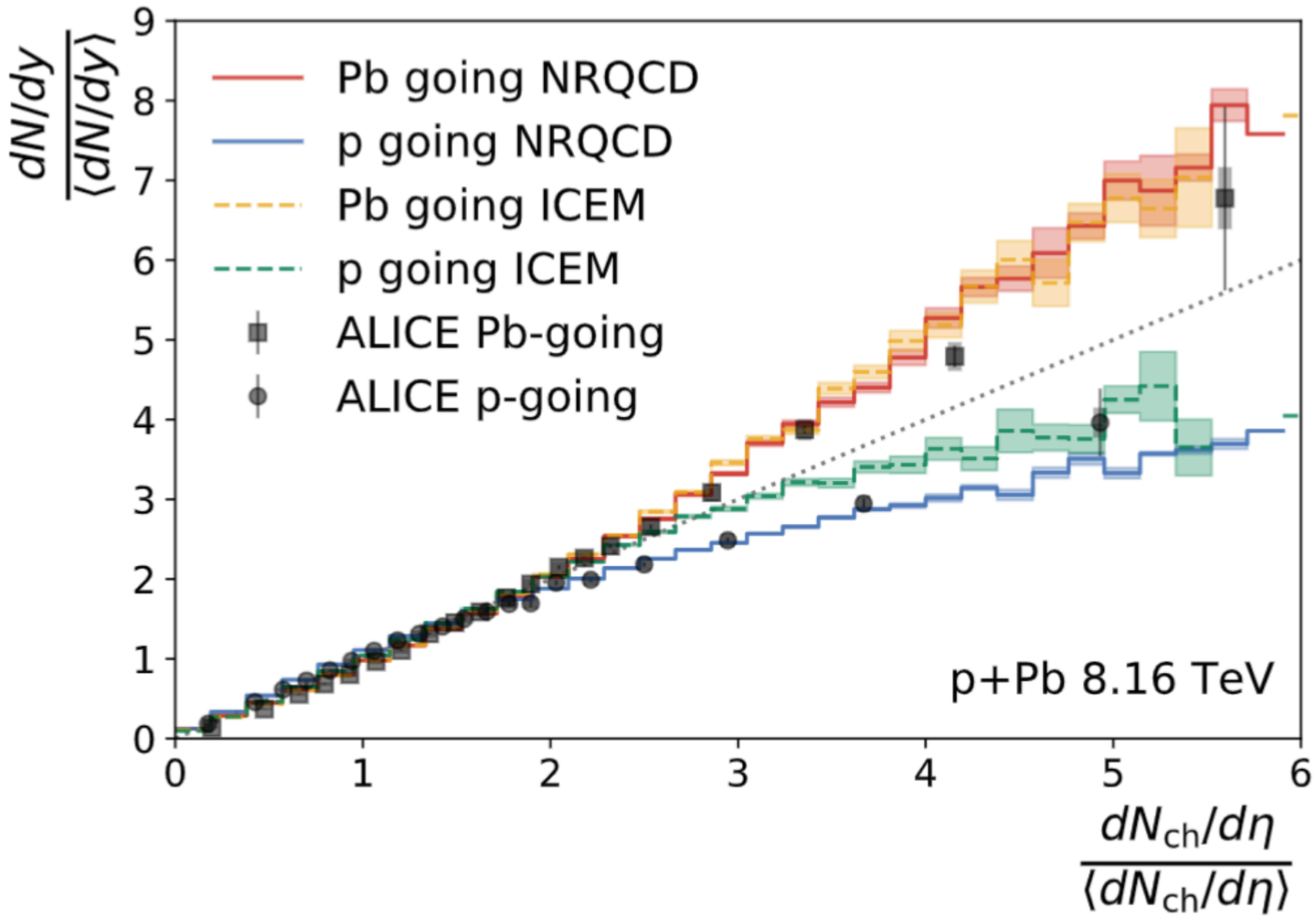

ICEM and NRQCD compatible in the backward region, but differ in the forward region where the former leads to less suppression

Quarkonium production in eA

- Studies of quarkonium production in DIS at small-x have focused mostly on diffraction, and employ a non-perturbative model for the light-cone wavefunction of quarkonium

- Our goal: Employ CGC + NRQCD to study the nuclear modification factor of quarkonium production in DIS

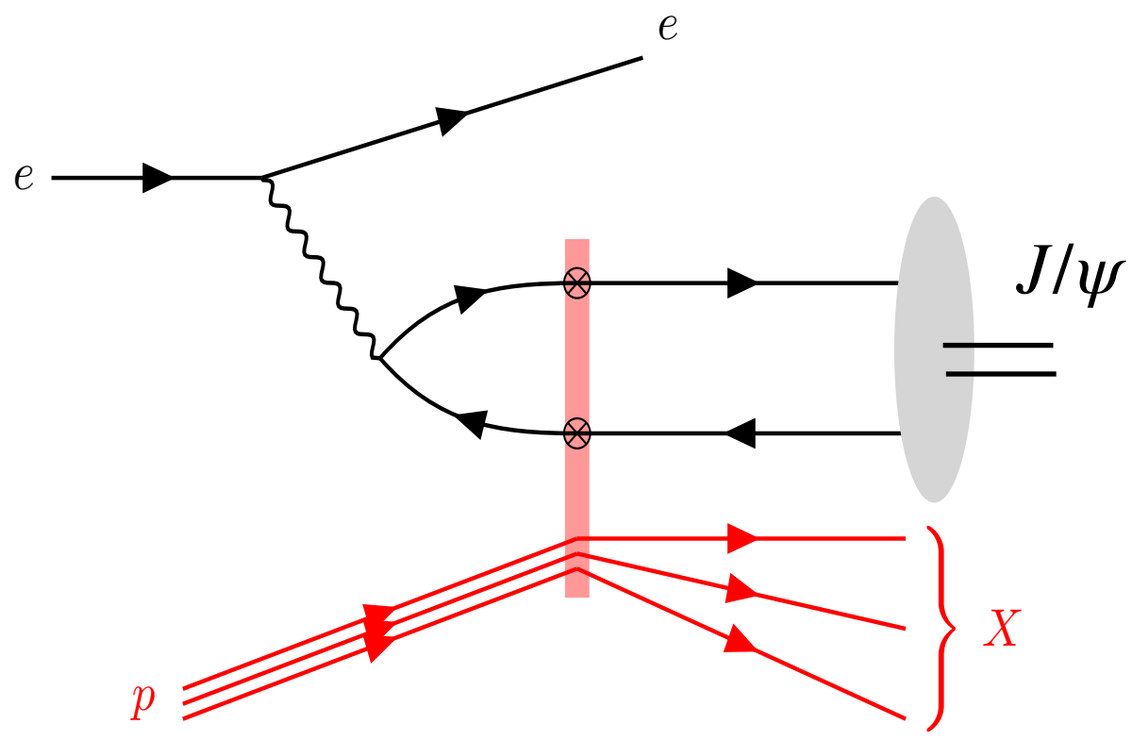

In progress Vincent Cheung, Zhongbo Kang, FS, and Ramona Vogt.

Potential future projects:
CGC+ICEM, quarkonium in UPCs, polarization observables and quarkonium production at NLO

Summary

- Quarkonium production in pp and pA collisions

  CGC + NRQCD/ICEM provide successful descriptions of rapidity and $p_\perp$ distribution, nuclear modification ratio, etc in high-energy pp and pA collisions at RHIC and LHC

- Multiplicity-dependent J/ψ distribution

  Sub-nuclear fluctuations in hotspots size and saturation scale provide a natural framework to generate different multiplicity classes that describe well LHC data

- Quarkonium production in eA

  Production cross-section using CGC + NRQCD will come soon with applications to the EIC

Back-up (tables)

Only four LDMEs contribute to J/ψ production: three for the color octet state $\langle \mathcal{O}^{J/\psi}_{^1S_0^{[8]}} \rangle = 0.089$ GeV^3, $\langle \mathcal{O}^{J/\psi}_{^3S_1^{[8]}} \rangle = 0.0030$ GeV^3, and $\langle \mathcal{O}^{J/\psi}_{^3P_0^{[8]}} \rangle / m_c^2 = 0.0056$ GeV^3, and one for the color singlet: $\langle \mathcal{O}^{J/\psi}_{^3S_1^{[1]}} \rangle = 1.16/(2N_c)$ GeV^3 [45, 46].

Parameter	Value	Parameter	Value
N_q	3	α_s	0.16
B_{qc}	3 GeV^{-2}	$m_{\rm IR}$	0.2 GeV
B_q	1 GeV^{-2}	$m_{J/\psi}$	3.1 GeV
σ_{B_q}	0.7	m_c	$m_{J/\psi}/2$
$\sigma_{Q_s^2}$	0.1	m_D	1.87 GeV
$S_\perp$	13 mb		

Table I. Standard set of parameters used. To constrain the normalization of multiplicities we use the experimentally determined inelastic cross section $\sigma_{\rm inel} = 2161$ mb for $\sqrt{s} = 8.16$ TeV p+Pb collisions (extrapolated from result at 5.02 TeV [64]), and $\sigma_{\rm inel} = 60$ mb for 7 TeV p+p collisions [65].

System	$\sqrt{s_{\rm NN}}$ [TeV]	J/ψ rapidity range	J/ψ rapidity used
p+p	7	$\lvert y\rvert < 0.9$	0
		$2.5 < y < 4$	3.03
p+Pb	5.02	$-4.46 < y < -2.96$	-3.52
		$-1.37 < y < 0.43$	-0.47
		$2.03 < y < 3.53$	2.62
	8.16	$-4.46 < y < -2.96$	-3.52
		$2.03 < y < 3.53$	2.62

Table II. Kinematic configurations of the experimental data presented in [8, 12, 66], and rapidity values used in our calculations. p-going: $y > 0$, small x in the Pb nucleus, large x in the proton; Pb-going: $y < 0$, large x in the Pb nucleus, small x in the proton.

Rapidity	p/Pb	Q_s [GeV]
midrapidity	p	1.35
	Pb	2.41
p-going	p	0.78
	Pb	4.18
Pb-going	p	2.78
	Pb	1.18

Table III. Typical values of Q_s in the proton and lead nucleus (in the region around the impact parameter) for $dN_{\rm ch}/d\eta = 4\langle dN_{\rm ch}/d\eta \rangle$.

For references see: FS, Schenke, Soto-Ontoso
[PLB 827 (2022) 136952]